Fizika Nizkikh Temperatur, 2000, v. 26, Nos. 9/10, p. 972–980

Experimental analysis of $^{13}CO_2$ infrared stimulated emissions in solid argon

H. Chabbi, P. R. Dahoo[1], H. Dubost[2], B. Gauthier-Roy, A.-M. Vasserot, and L. Abouaf-Marguin

Laboratoire de Physique Moléculaire et Applications du CNRS, associé à l'Université Pierre et Marie Curie, Tour 13, boite 76, 4 place Jussieu, 75252 Paris Cedex 05, France
E-mail: la@ccr.jussieu.fr

Received March 10, 2000

Vibrational stimulated emissions of CO_2 trapped in low temperature argon matrices have been found experimentally not only in the 16 μm region (ν_2 manifold) but also at 10 μm ($\nu_3 - \nu_1$ transition) in the double trapping site of concentrated samples. A detailed experimental description of these emissions is reported, including spectral analysis, time-resolved studies, laser energy dependence, and concentration and temperature effects. The characteristics of the emissions are discussed, giving some insight into the nonradiative intramolecular V–V transfers from the laser excited level $\nu_3 = 1$ towards the ν_2 manifold, and inside this manifold.

PACS: **78.45.+h**, **78.30.–j**, **34.30.+h**

Introduction

Recently [1–3] we have shown that low-temperature matrices offer favorable conditions for the observation of vibrational stimulated emission. Excitation by an infrared laser pulse leads to large population inversions among the vibrational levels of the guest molecules so that the matrix becomes an amplifying medium at the corresponding frequencies. Spontaneously emitted photons are then amplified on their passage through the sample, a phenomenon usually called amplified spontaneous emission [4,5] (ASE). When it originates from a vibrational transition, the process is also referred to as IRSE (infrared stimulated emission) or VSE (vibrational stimulated emission). This phenomenon only happens if the population of excited molecules exceeds a threshold, which discriminates between stimulated and spontaneous processes. When compared to spontaneous emission, a VSE signal appears amplified and shortened by a factor which can reach several orders of magnitude, depending on numerous factors such as the linewidth and line strength of the transition, density of excited molecules, thickness of the sample, and temperature. The amplified pulse should be followed by the spontaneous fluorescence of the molecules, whose population inversion has decreased to under threshold. This has been observed, for example, in the case of CO trapped in a mercury doped nitrogen matrix [6]. The stimulated peak is about 150 times larger than the maximum of the remaining long fluorescence, and it is only observed in a narrow temperature interval (17–22 K). In most experiments [1–3], on the contrary, we detect a giant pulse without any longer spontaneous signal, this fluorescence being obviously too weak for the sensitivity of our detection. Among the three triatomic molecules recently studied, $O_3^{[1]}$, $CO_2^{[2]}$, and $N_2O^{[3]}$, CO_2 provides the reachest system due to the rather long time scale of the 16 μm emissions. Moreover, these emissions arise from different vibrational levels in the ν_2 manifold.

The aim of the present paper is to complete the preliminary results [2] by a thorough experimental

Present address: [1] Laboratoire de Magnétisme et d'Optique de Versailles, Bâtiment Fermat, 45 avenue des Etats-Unis, 78035 Versailles, France
[2] Laboratoire de Photophysique Moléculaire du CNRS, Bâtiment 213, Université de Paris-Sud, 91405 Orsay Cedex, France

study involving spectroscopic details, time analysis, and concentration and temperature effects. Besides, a new result has been obtained: we have found stimulated emission also in the 10 μm region.

Experimental setup

Details about the apparatus and experimental procedures can be found in Refs. 1 and 7. We briefly recall here the main features. Solid argon samples are obtained by deposition of a gaseous mixture onto a gold plated copper mirror held at 18 K in a liquid helium cryostat. The sample thickness is known from the amount of gaseous mixture used during the deposition. A calibration of the thickness vs. the deposited He–He laser recorded during growth of the sample. The sample is then cooled to 5 K. Carbon and platinum resistors measure the temperature, which can be varied between 5 and 30 K. The concentration of the CO_2/Ar mixture is chosen in the range 1/200–1/10000. The infrared excitation pulse is obtained by frequency difference between a dye laser (pumped by a frequency doubled YAG laser) and the YAG residual. The system, purchased from Quantel (France), generates pulses of 200 μJ maximum energy, 5 ns time width, and 0.8 cm^{-1} spectral width. The repetition rate is 20 Hz. The laser, focused on an area of $2\cdot 10^{-2}$ cm^2, impinges normally on the sample mirror. The detection angle, usually 45°, can be varied by ± 8°. Signals are detected using an MCT detector (Belov Technology) and accumulated in a digital oscilloscope (Tektronix TDS 540). A high-pass filter (λ_c = 8 μm) is used to get rid of the scattered laser light. Absorption spectra of the sample are recorded using a Bruker IFS 113V FTIR spectrometer with a maximum resolution of 0.03 cm^{-1}. Emissions are spectrally analyzed by means of filters, or through a Perkin-Elmer monochromator equipped with a 16 μm blazed grating (60 lines/mm). The effective resolution is a few cm^{-1}.

Experimental results

1. Spectral analysis

1a) Absorption spectroscopy. It is now well known from experimental work [8] and from calculations [9] that argon matrices offer two different trapping sites to the CO_2 molecule. The more stable one is unambiguously assigned to a single substitutional site, where the molecular axis coincides with the C_4 symmetry axis of the site. The other site is «unstable», which means that the absorption by molecules in this site decreases irreversibly upon annealing. It is described as a more or less distorted double substitutional site, where the molecule is placed asymmetrically, which results in the lifting of the ν_2 mode degeneracy. For a quantitative study of stimulated effects, we need linewidth values for CO_2 in our experimental conditions, namely after deposition at 18 K, a temperature chosen a little lower than usual in order to favor the double site, so that the same detection conditions can be used for the two sites. Then at 5 K we recorded, with our best resolution, the absorption spectra of unannealed samples similar to those studied in emission experiments. The ν_2 region is displayed in Fig. 1: the low-frequency line (FWHM $= 92\cdot 10^{-3}$ cm^{-1}) belongs to the single site. The high-frequency doublet (FWHM = $38\cdot 10^{-3}$ and $30\cdot 10^{-3}$ cm^{-1}) is assigned to the double site. Two very narrow extra lines, which do not decrease upon annealing, cannot be confused with the double site monomer absorption, and we tentatively assign them to a dimer. These assigments rest upon irreversible annealing effects: heating the sample up to 32 K, during a few minutes, results in an increase of the two small lines at 644.6 and 644.8 cm^{-1} (dimer ?), whereas the 643.2 isolated line decreases by 5% (monomer, stable site) and the 644.5–645.0 cm^{-1} doublet decreases by 23% (monomer, unstable site). The measured linewidths are consistent with those obtained [10] with a resolution of 0.010 cm^{-1} for $^{12}CO_2$ in argon deposited at 20 K (FWHM = $= 75\cdot 10^{-3}$, $29\cdot 10^{-3}$, and $25\cdot 10^{-3}$ cm^{-1}, respectively, at 5 K). In the ν_3 region, which will be used for excitation, we measure linewidths of 0.36 and 0.12 cm^{-1}, respectively, for the single and double sites.

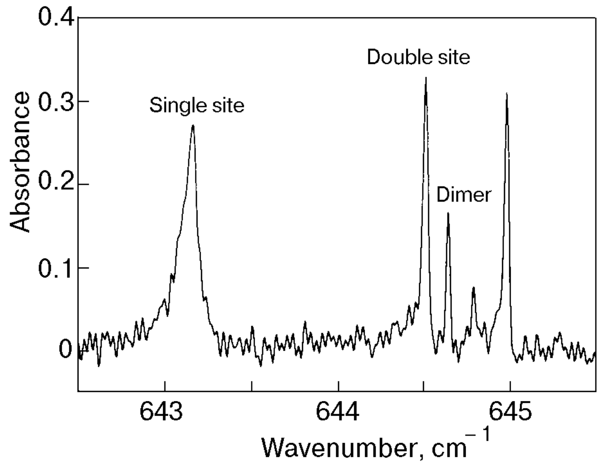

Fig. 1. FTIR absorption spectrum of $^{13}CO_2$ in solid argon at 16 μm (CO_2/Ar = 1/2300, T = 5 K, thickness ≈ 13 μm, resolution = 0.03 cm^{-1}).

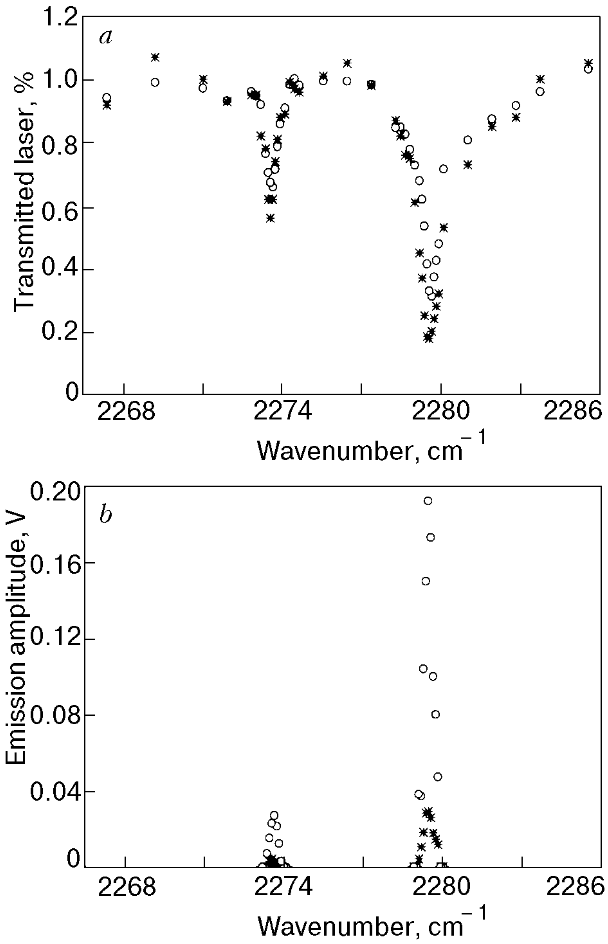

Fig. 2. Spectral analysis of the excitation for laser energies 50 (*) and 77 μJ/pulse (○) (CO_2/Ar = 1/2000, T = 5 K, thickness ≈ 90 μm). Transmission spectrum of the laser, at incidence 45° (*a*); excitation spectrum of the 16 μm emission, detected at incidence 0° (*b*).

1b) Absorption of the exciting laser by the ν_3 *mode*. Specific experiments have been performed to get the number of photons absorbed from the laser, tuned through the ν_3 region: the laser is presently incident at $i = 45°$ and the transmitted energy is collected after reflection on the sample mirror, so that the absorption length is equal to the thickness of the sample multiplied by $2\sqrt{2}$. As the ν_3 transition of CO_2 is very intensive, saturation of the absorption may occur, especially for dilute samples, which can be checked by comparing the «laser transmission spectrum» recorded point by point, for different laser energies. We emphasize that by this procedure the laser width and the molecular linewidth are automatically taken into account. Moreover, an additional detector is placed at $i = 0°$ in order to monitor the emission, thus providing the corresponding excitation spectrum. This has been done at the concentration of 1/2000 for different sample thicknesses. Figure 2 displays the results for a 90 μm thick sample and clearly shows saturation effects, which means that, at least in the first layers, at high energy, the percentage of excited molecules approaches 50%. This had been predicted in Ref. 2 and is now quantitatively established. Doubling the thickness decreases the saturation effect appearing on the spectrum, which only gives a mean value of the excited population, as the excitation is not homogeneous all over the sample. The perfect correlation between the emission and the absorption is clearly established for the two sites.

Besides, this experiment allows an additional observation concerning the absence of directionality of the emission. As a matter of fact, the detector, without a lens and remaining at a constant distance from the sample, sees a constant signal (largest deviation = 16%) when the direction of observation is moved between 0 and ± 10°. Going back to the usual geometry, with the laser beam coming in normally to the mirror, and moving the detection to 45 ± 8°, also gives an equal signal within the same precision. As the absorption length is now reduced by a factor of $\sqrt{2}$, there is a little, if any, increase of the emission efficiency when the observation angle is increased.

1c) Emissions in the 10 and 16 μ*m regions*. In the N_2O case [3] the $\nu_3 - \nu_1$ transition, originating from the laser-excited $\nu_3 = 1$ level, is the only transition observed, i.e., amplified by stimulated emission. It was not observed for CO_2/Ar samples of similar concentration (1/2000) and similar thickness (90 to 260 μm). It was searched for, and found, at higher concentrations (1/500 and 1/200) but coming only from molecules in the double site. With the 60 lines/mm grating, we cannot observe 10 μm radiation through the monochromator. We then characterize the 10 μm emission by CaF_2 or BaF_2 plates absorbing at 16 μm. A 5 mm thick CaF_2 plate decreases the emission by a factor of 1/3. The emission is highly unstable, which makes its detection tricky. Only single shots are meaningful. Even when optimization is achieved, and for large laser shots, the emission intensity is random. Figure 3,*a* displays a particularly strong single shot signal detected through a BaF_2 window. Replacing the BaF_2 by a high-pass filter (λ_c = 13 μm) allows the detection of the 16 μm emission already described in Ref. 2, which is shown in Fig. 3,*b*. Figure 3,*c* displays the total signal, only through an 8 μm high pass filter to eliminate the scattered laser light. The trace presented in Fig. 3,*b* is shown in heavy shading in Fig. 3,*c* to recall its contribution to the total signal.

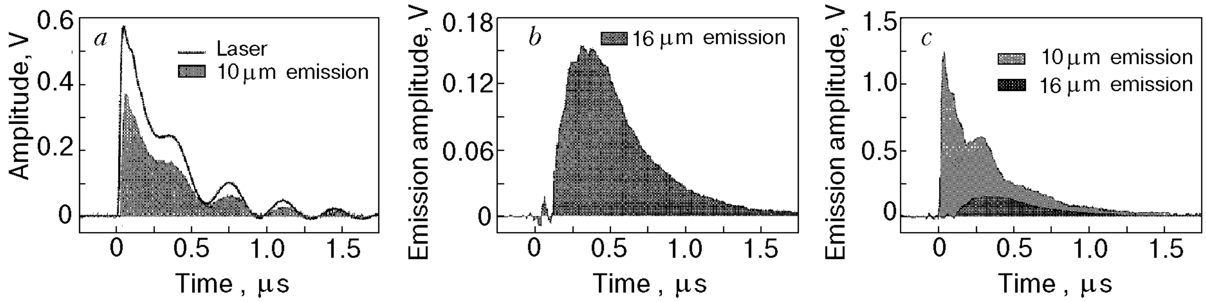

Fig. 3. Discrimination between 10 μm and 16 μm emissions by means of filters (CO_2/Ar = 1/525, T = 5 K , thickness ≈ 40 μm). Detection through a BaF_2 plate (*a*); detection through a λ_c = 13 μm high-pass filter (*b*); detection without filter (*c*). In each case, except to record the laser, a λ_c = 8 μm high-pass filter eliminates the scattered laser light.

Using the BaF_2 plate, we checked the lack of directionality of the 10 μm emission, and found that it is not polarized, just as was found for the 16 μm emission. The 16 μm emission, analyzed through the Perkin-Elmer monochromator, exhibits three lines for each site, shifted by 1 cm^{-1} in wavenumber from one site to the other. The measured wavenumbers (626, 613, and 595 cm^{-1}) allow their unambiguous assignment to combination bands inside the ν_2 manifold as is shown in Fig. 4. The lines at 626 and 595 cm^{-1} are identified with the $11^10(2) \to 10^00(2)$ and $11^10(2) \to 02^20(1)$ transitions, whereas the 613 cm^{-1} emission comes from the $10^00(2) \to 01^10(1)$ transition. The fundamental ν_2 transition at 644 cm^{-1} has been searched for without success.

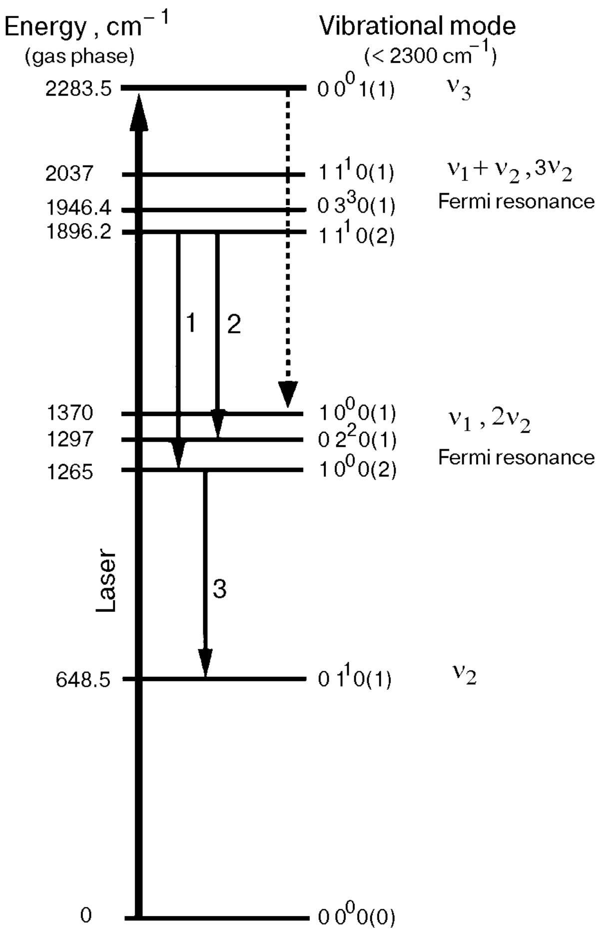

Fig. 4. Vibrational energy levels of $^{13}CO_2$ up to 2300 cm^{-1}. 1, 2, 3: 16 μm emissions (——) and 10 μm emission (- - -).

2. *Time analysis*

2a) 10 μm emission. Short-time measurements are limited by the characteristics of the detection. The apparent half-width of the 5 ns laser pulse, reaching about 400 ns, is shown in Fig. 3,*a*, where the laser is recorded in the absence of absorption and without any filter. The 10 μm emission appears with a delay too small to be measured. Both decays, identical, reflect the time constant of the system.

2b) 16 μm emissions. On the contrary, a measurable delay is found for the onset of the 16 μm emissions. Their time shape is clearly different from the laser one, as detected through the monochromator in the fourth order of the grating (Fig. 5). This time analysis of the dispersed emission reveals that the three lines of the two sites have different time behaviors. The onset and the signal maximum are reached faster in the single site than in the double one. Moreover, for a given site, the three lines exhibit a different time delay, and they have been numbered according to this delay. Last but not least, the 613 cm^{-1} emission (line *3*) of the double site shows a peculiar, rather intricate, time behavior. An intense peak, on a short time scale similar to that for the other two lines, is followed by a much weaker and longer component, covering a few tens of microseconds.

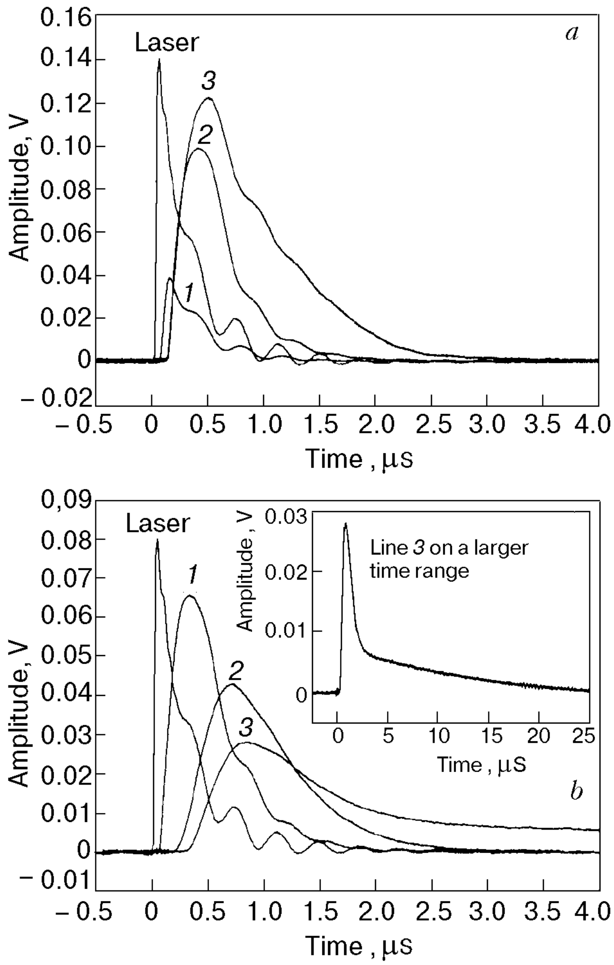

Fig. 5. Time and frequency resolved 16 μm emissions (CO_2/Ar = 1/2000, T = 5 K, thickness ≈ 360 μm): single site (*a*) and double site (*b*).

3. Threshold measurements

The dependence of the emission amplitude on laser energy is shown for each transition in Figs. 6 (single site) and 7 (double site).These data correspond to 360 μm thick samples at concentrations of 1/2000 and 1/500 for the 16 and 10 μm emissions, respectively. Below a sharp energy threshold, depending on the transition, no signal is usually detected. Above the threshold the dependence seems approximately linear in the studied range, as was observed in the O_3 [1] and N_2O [3] cases. The existence of such a threshold gives direct evidence of the stimulated character of the process, in addition to the large amplification and shortening effects relative to spontaneous fluorescence.

The $2\nu_2^0 - \nu_2^1$ transition at 613 cm^{-1} (line *3*) behaves peculiarly in the two sites. In the double site, the short component exhibits a sharp threshold at 115 μJ, whereas the longer one, with a much weaker amplitude, shows a slower decrease. Finally, it disappears into noise, and it is impossible to measure a precise threshold different from zero. The stimulated or spontaneous character of this component is then not established. For the single site, Fig. 5 does not show two distinct time components for this transition. However, at high laser energy, the delay of this emission is smaller and its width (FWHM) is broader, as if a short component of similar amplitude was added at the beginning of the signal. This observation may be used to discuss the two regimes appearing in Fig. 6,*c*. A high threshold of 100 μJ is assigned to the additional short part, the global threshold being lower, at 40 μJ.

The threshold value measured for each component is an essential parameter for any quantitative discussion, provided that the laser absorption is known. To sum up, the present results are the

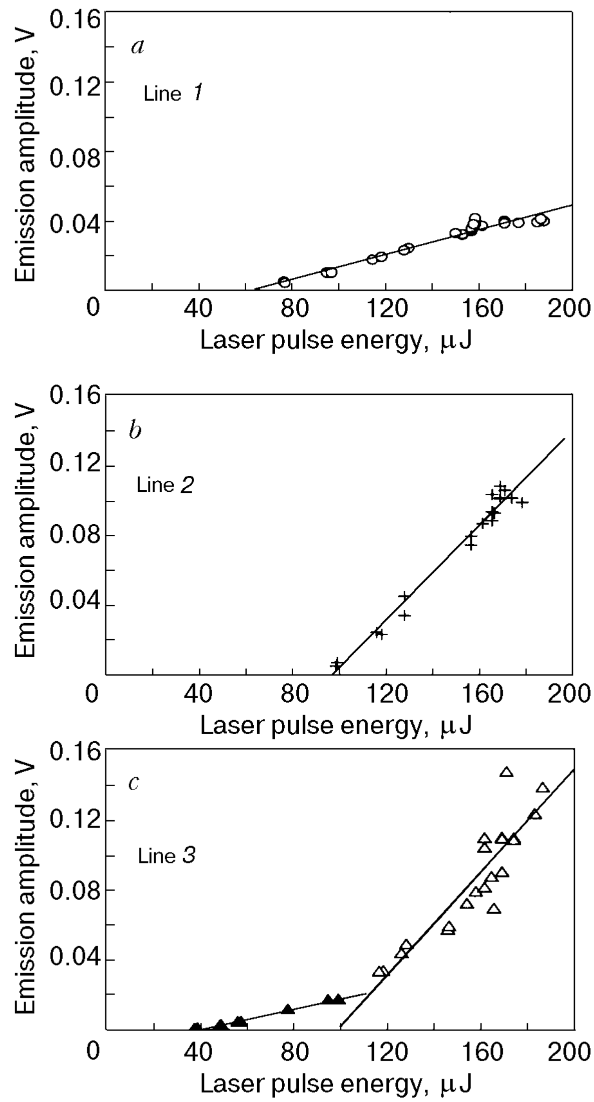

Fig. 6. Dependence of the emission amplitude on the laser pulse energy (T = 5 K, sample thickness ≈ 360 μm, single site), 16 μm emissions, CO_2/Ar = 1/2000, line *1* (○); line *2* (+); line *3*, short and long components (Δ and ▲, respectively).

following: threshold values of 65, 97, 100 (and 40) μJ are found for lines *1*, *2*, and *3*, respectively, in the single site, which absorbs about 86% of the laser energy. The corresponding values for the double site (Fig. 7) are 80, 110, and 115 μJ, with an absorption around 50%. Figure 7,*d* yields a threshold of 120 μJ for the 10 μm emission from a sample of similar thickness, but with a concentration increased by a factor of 4, resulting in an evaluated absorption of the order of 94%.

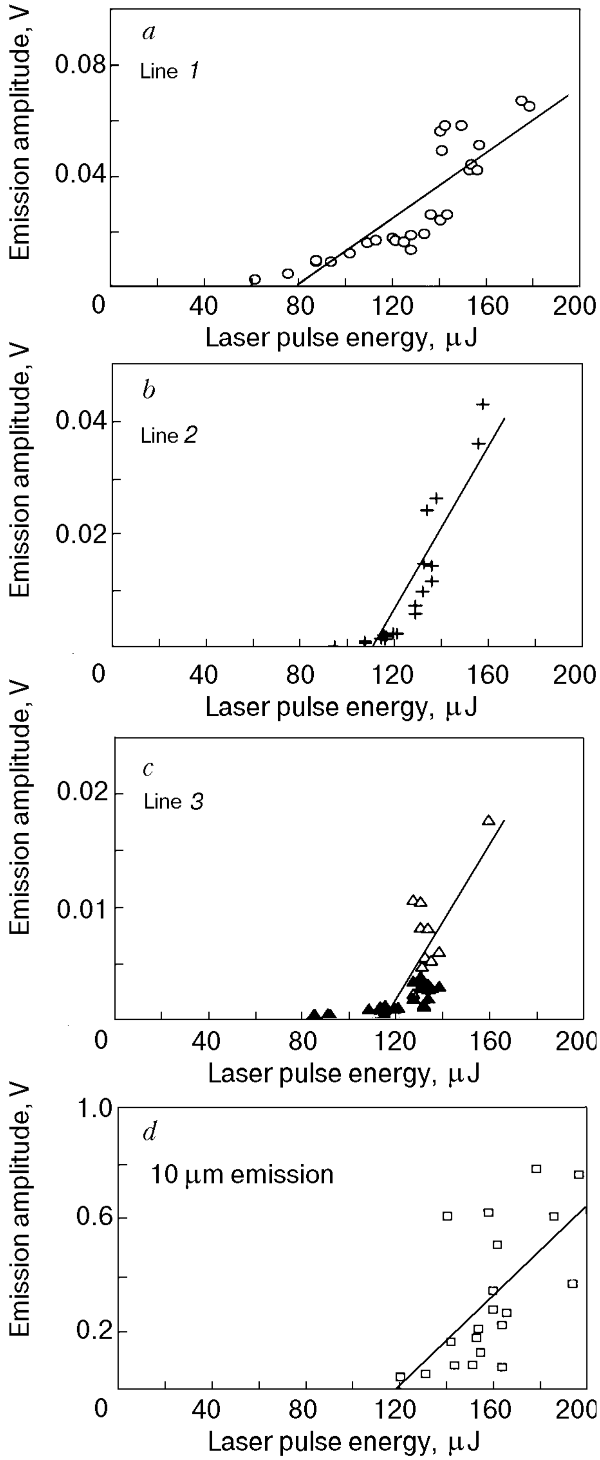

Fig. 7. Dependence of the emission amplitude on the laser pulse energy (T = 5 K, sample thickness ≈ 360 μm, double site), 16 μm emissions, CO_2/Ar = 1/2000: line *1* (❍), line *2* (+), line 3, short and long components (Δ and ▲, respectively); 10 μm emission, CO_2/Ar = 1/520 (❒).

4. Concentration and temperature effects

The most important concentration effect is the appearance of the 10 μm emission of the double site for concentrations higher than 1/1000. On the contrary, in this case, the 16 μm emission is weaker than for the concentrations of 1/1000 and 1/2000. In this range the 16 μm signals are maximum, if one compares samples of approximately equal optical density, i.e., keeping constant the product of the concentration by the thickness. Of course, a concentration decrease from 1/2000 to 1/10000 also decreases the signals, since we cannot grow samples thick enough to keep the optical density constant. We focus our attention on the concentration dependence of the long component of line *3* in the double site, because it could be assigned to spontaneous emission from its time behavior and its threshold uncertainty. We unsuccessfully tried exponential fits of its decay. However, a time constant extracted from its last part shows an unusual concentration dependence, as it clearly decreases with increasing dilution.

Another way to characterize the time behavior of this component is to decrease the laser energy below the threshold of the short component. We thus observe an onset, a maximum and a decay, and an approximate value of the time during which the signal remains higher than the noise. Once again, this time clearly decreases with increasing dilution.

Temperature effects can be studied up to 30 K only for the single site, since the density of double sites decreases irreversibly upon annealing. For the single site, increasing the temperature from 5 to 17 K results in an increase of line *1* by about 35%, including a very little increase in duration, measured by its full width at half maximum (FWHM). Between 17 and 21 K this line remains approximately constant. It disappears at 28 K. On the contrary, lines *2* and *3* keep on decreasing from 5 to 21 K. Their amplitude and width decrease together, and they disappear at 22 K (line *3*) and 23 K (line *2*). At 5 K, after this temperature cycling, the emissions of the three lines are increased by about 40% (line *1*) and more than 60% (lines *2* and *3*). This effect may be explained by a narrowing of the lines due to annealing.

For the double site, the temperature dependence studied up to T = 21 K is approximately similar.

Lines *2* and *3* decrease and disappear at 20 and 19 K, respectively, whereas line *1* is nearly constant. Moreover, such a mild temperature cycling also produces an overall increase of the emissions at $T = 5$ K, very likely related to a line narrowing.

Discussion

1. Inversion population thresholds for ASE

ASE is considered to start as soon as one spontaneous photon produces a stimulated photon on its passage through the sample. Defining a mean path length $\langle \mathbf{l} \rangle$ as the mean distance from any point to the boundaries of the excited volume, this condition can be written as

$$\sigma_{ul} \Delta N_{ul} \langle \mathbf{l} \rangle \geq 1 \ , \tag{1}$$

where σ_{ul} [cm^2] is the cross section for stimulated emission from upper level u to lower level l, and ΔN_{ul} [cm^{-3}] is the population inversion between these two levels. Equivalently, one can define a loss coefficient $\alpha_L = 1/\langle \mathbf{l} \rangle$ and write

$$\sigma_{ul} \Delta N_{ul} - \alpha_L \geq 0 \ . \tag{2}$$

The threshold condition for the population inversion ΔN_{ul}^T is then

$$\sigma_{ul} \Delta N_{ul}^T = \alpha_L \tag{3}$$

with

$$\sigma_{ul} = \frac{8\pi^3}{3hc} \frac{\nu_{lu}}{\gamma_{lu}} |R_{lu}|^2 \frac{1}{n} \left(\frac{n^2 + 2}{3} \right)^2 ; \tag{4}$$

σ_{ul} mainly depends on molecular parameters, such as the squared transition moment $|R_{lu}|^2$, the wavenumber ν_{lu} , and the linewidth γ_{lu} of the transition. It is also related to the nature of the matrix by its refractive index n, but does not depend on the geometry of the sample. On the contrary, α_L is essentially related to the thickness of the sample and the diameter of the laser-excited spot. Consequently, we can compare threshold population inversions ΔN_{ul}^T for different transitions provided that the matrix and the geometry of the sample are not changed. This can be performed at a semi-quantitative level, taking the next gas phase values [11–13] for $|R_{lu}|^2$: $1.77 \cdot 10^{-3}$, $0.67 \cdot 10^{-3}$, $50.6 \cdot 10^{-3}$, $20.3 \cdot 10^{-3}$, and $21.9 \cdot 10^{-3}$ Debye [2] for the transitions $\nu_3 - \nu_1$, $\nu_3 - 2\nu_2$, $3\nu_2^1 - 2\nu_2^0$, $3\nu_2^1 - 2\nu_2^2$, and $2\nu_2^0 - \nu_2^1$, respectively. The $|R_{lu}|^2$ values of the 10 μm transitions are one or two orders of magnitude smaller than the 16 μm ones, which explains why detection of 10 μm emission requires higher concentrations, although the emitting level is directly laser excited.

For the linewidths γ_{lu} , which cannot be measured at the solid argon temperature for combination or hot bands, we tentatively use the values measured in the present study for the corresponding fundamentals. The measured thresholds displayed in Fig. 6 for the emissions of the double site can be analyzed within this approximation. First, considering the 10 μm emission, we can safely assign it to the $\nu_3 - \nu_1$ transition on the basis of the $|R_{lu}|^2$ values, which makes the $\nu_3 - 2\nu_2$ threshold higher by a factor of 2.6. A calculated value of $64 \cdot 10^{-19}$ cm^2 is found for the cross section σ_{ul} of the $\nu_3 - \nu_1$ emission. Using the threshold energy, and the estimated absorption of 94%, we get the inversion population threshold $\Delta N_{ul}^T \cong 0.37 \cdot 10^{19}$ cm^{-3}. We then obtain $\alpha_L \cong 24$ cm^{-1} for the loss coefficient. This value is somewhat too high for a 360 μm thick sample, when compared to the value of 26 cm^{-1} determined using the 10 μm emission of N_2O [3] in a 180 μm thick sample. Taking into account how $\langle \mathbf{l} \rangle$ depends on the thickness, if one neglects light scattering, we would have predicted $\alpha_L \cong 18$ cm^{-1}. Nevertheless the order of magnitude is correct. More interesting is the comparison with the other emissions in similar samples. The value $\alpha_L = 24$ cm^{-1} allows a prediction of ΔN_{ul}^T equal to $9.5 \cdot 10^{16}$, $25 \cdot 10^{16}$, and $23 \cdot 10^{16}$ cm^{-3} for lines *1*, *2* and *3*, respectively. Let us compare these values with the experimental threshold values of the $\nu_3 = 1$ level population, $110 \cdot 10^{16}$, $180 \cdot 10^{16}$, and $180 \cdot 10^{16}$ cm^{-3}, respectively. This shows that only about 10% of the molecules have relaxed from the $\nu_3 = 1$ level towards the $3\nu_2$ one, when ASE starts in the ν_2 manifold. Using the delay of line *1* (~ 70 ns) we get an order of magnitude value $k = 3 \cdot 10^7$ s^{-1} for this intramolecular V–V transfer rate in the double site.

2. Low directionality of the emissions

In the experimental Section, we established that the emissions exhibit low directionality. This observation is in contradiction with the high directionality predicted for ASE in the gas phase [4,5], where the length of the amplifying medium is a crucial parameter. In the present experiment, the excited part of the sample is a disk about 200 μm thick and 1.5 mm in diameter, so that the preferential emission direction should be in the plane of the disk. However, in the matrix case, light scattering by the polycrystalline material, for both excitation and emission, provides random propagation directions as well as random optical path lengths. The low directionality of the emission, which is proven here, can then be understood.

3. *Time behavior of the emissions and relaxation scheme*

The 10 μm emission reproduces almost exactly the laser pulse, within the response time of the detection. This is not surprising, since this emission comes from the level $\nu_3 = 1$ directly excited by the laser and was observed also in the N_2O case. This does not provide any information on the lifetime of this level, since ASE itself decreases the population below threshold.

For the 16 μm emissions, it is surprising that two signals (lines *1* and *2*) exhibit such different time behaviors even though they come from a common level ($3\nu_2^1$), which is populated via intramolecular V–V transfer from the $\nu_3 = 1$ level. One easily understands that the threshold for ASE is reached faster for the transition with the higher transition moment (line *1*). But we have to explain why the onset of line *2* coincides with the decay of line *1*, although the emitting population is the same for the two lines. Moreover, in the double site, line *1* is the more intense, while in the single site the reverse is true. Let us consider the level scheme displayed in Fig. 4. ASE operating on line *1* tends to equalize instantaneously the populations of the upper and lower levels, resulting in saturation of the gain. If the relaxation of the lower level is not fast, both populations increase as the transfer $\nu_3 \rightarrow 3\nu_2^1$ goes on. Such a process has been described by Apkarian [14] using a kinetic model for a two-level system. The emitted signal exhibits oscillations on a very short time scale, corresponding to a step-by-step increase of the lower level population. When the $3\nu_2^1$ population reaches the threshold for ASE on line *2*, the dominant process changes. Indeed, a well known «energy gap law» [15] for multiphonon vibrational relaxation in matrices states that the nonradiative rates decrease exponentially with the number of phonons to be created for energy conservation. One can then safely assume that the lower level of line *2* ($2\nu_2^2$) relaxes faster than that of line *1* ($2\nu_2^0$) because of the small energy difference between these two levels as compared to the gap of 613 cm^{-1} between $2\nu_2^0$ and ν_2^1. Consequently, the gain of the amplifying medium on line *2* does not saturate, since there is no equilibration of the populations. Moreover, ASE on line *2* contributes to the population of the lower level of line *1*, which qualitatively explains why, when line *2* is on, line *1* is off. The relative intensities of lines *1* and *2*, going from one site to the other, is probably explained by differences between the nonradiative rates populating $3\nu_2^1$. In the double site, where the molecule has a wider space, it is probably less coupled to the phonon bath, so that all rates are smaller. This is consistent with the longer delay before the onset of the three lines. This effect may be different for the different nonradiative transfer rates. A clue confirming this interpretation is provided by the temperature effect. When heating the matrix, the V–V nonradiative transfer rates generally increase. Saturation of the gain on line *1* is decreased by the faster relaxation of the lower level $2\nu_2^0$. Line *1* is then favored. Moreover the nonradiative relaxation of level $3\nu_2^1$ is also faster. The two channels (radiative and nonradiative) that depopulate $3\nu_2^1$ are then increasing. This explains the decrease of line *2*, until finally its threshold cannot be overcome. The delay observed for the onset of line *3* reflects the time necessary for the different transfers (radiative and nonradiative) to provide the threshold population inversion of line *3*. A quantitative rationalization of the time evolution of the emissions would imply a complete kinetic model, inspired by that of Apkarian [12] but taking into account the whole ν_2 manifold instead of a two-level system, and including the nonradiative V–V transfers between all the involved levels. This model may allow an estimation of the transfer rates.

4. *Concentration behavior of line 3 in the double site: stimulated or spontaneous emission?*

When recording spontaneous emission, one has a direct access to the lifetime of the emitting level. In matrices, due to possible intermolecular V–V transfers towards impurities or dimers, occurring at high concentration, it is generally observed [16] that the lifetimes increase with increasing dilution, up to a limit where the molecules can be considered as

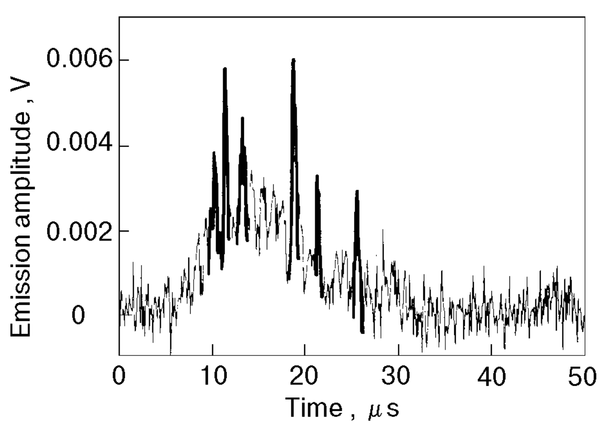

Fig. 8. Single-shot record of line *3*, just below the threshold of its short component (T = 5 K, CO_2/Ar = 1/2000, sample thickness ≈ 260 μm, double site).

perfectly isolated in the lattice. One then gets the intrinsic lifetime of the level, as governed by the interaction of the molecule with the lattice. The concentration dependence observed for line *3* and abovementioned does not fit in with such a scheme. This unusual dependence proves that the signal does not yield the $2\nu_2^0$ lifetime. There must remain some stimulated effect, even under threshold, spoiling the lifetime measurements. Indeed, a single-shot record of this long component, around the threshold, exhibits random bursts of stimulated emission (Fig. 8), which closely resembles the spiking often encountered in solid state lasers [17].

Nevertheless, the duration of line *3* emission proves that the $2\nu_2^0$ level remains populated after 20 μs (Fig. 5,*b*), which sets a higher limit ($\sim 10^5$ s^{-1}) for the intramolecular vibrational relaxation rates inside the ν_2 manifold. The kinetic model suggested in the preceding discussion should be able to shed more light on this question. It is presently in progress at L. P. M. A.

Conclusion

Vibrational emissions of $^{13}CO_2$ trapped in argon matrices have been studied in the 10 μm and 16 μm regions. They all behave like stimulated emission, even in the case of the long component of the $2\nu_2^0 - \nu_2^1$ transition, which lasts over some tens of microseconds. An order of magnitude value of $3 \cdot 10^7$ s^{-1} can be set for the nonradiative V–V transfer rate from the excited ν_3 level to the $3\nu_2^1$ level. Other intramolecular V–V transfers inside the ν_2 manifold have been discussed qualitatively. A quantitative estimate of these rates might be extracted from a kinetic model including spontaneous and stimulated emission and nonradiative transfers. Simulations based on this model are presently in progress.

1. D. Jasmin, P. Brosset, R. Dahoo, B. Gauthier-Roy, and L. Abouaf-Marguin, *J. Chem. Phys.* **108**, 2302 (1998).
2. H. Chabbi, P. R. Dahoo, B. Gauthier-Roy, A.-M. Vasserot, L. Abouaf-Marguin, M. Broquier, H. Dubost, R. Kolos, A. Tramer, J.-M. Berset, and J.-M. Ortega, *Chem. Phys. Lett.* **285**, 252 (1998).
3. H. Chabbi, P.R. Dahoo, B. Gauthier-Roy, A.-M. Vasserot, and L. Abouaf-Marguin, *J. Phys. Chem. A (in press)*.
4. L. Allen and G. I. Peters, *J. Phys.* **A4**, 238 (1971).
5. Y. Ogi and K. Tsukiyama, *Chem. Phys. Lett.* **296**, 384 (1998).
6. C. Crépin, F. Legay, N. Legay-Sommaire, and A. Tramer, *Opt. Commun.* **58**, 100 (1986).
7. D. Jasmin, P. Brosset, P. R. Dahoo, V. Raducu, B. Gauthier-Roy, and L. Abouaf-Marguin, *J. Chem. Phys.* **101**, 7337 (1994).
8. R. Guasti, V. Schettino, and N. Brigot, *Chem. Phys.* **34**, 391 (1978).
9. P.R. Dahoo, I. Berrodier, V. Raducu, J.-L. Teffo, H. Chabbi, A. Lakhlifi, and L. Abouaf-Marguin, *Eur. Phys. J. D* **5**, 71 (1999).
10. N. Legay-Sommaire and F. Legay, *Private communication*, L. P. P. M., Orsay, France (1999).
11. J.-Y. Mandin, V. Dana, M. Badaoui, G. Guelachvili, M. Morillon-Chapey, Q. Kou, R. B. Wattson, and L. S. Rothman, *J. Mol. Spectrosc.* **155**, 393 (1992).
12. J. W. C. Johns and J. Wander Auwera, *J. Mol. Spectrosc.* **140**, 71 (1990).
13. L. S. Rothman, R. L. Hawkins, R. B. Wattson, and P. R. Gamache, *JQSRT* **48**, 537 (1992).
14. V. A. Apkarian, *Chem. Phys. Lett.* **110**, 168 (1984).
15. V. E. Bondybey, in: *Chemistry and Physics of Matrix – Isolated Species*, L. Andrews and M. Moskovits (eds.), North Holland, Amsterdam (1989).
16. H. Dubost and F. Legay, in: *Chemistry and Physics of Matrix – Isolated Species*, L. Andrews and M. Moskovits (eds.), North Holland, Amsterdam (1989).
17. W. Koechner, *Solid-state Laser Engineering*, 4th edition, Springer, Berlin (1996).